

Enclosure 2

2CAN010402

**Wesdyne Report WDI-TJ-001-02-NP, Rev 02,
Detection of Reactor Head Base Metal Loss from Inside the CRDM
(Non-Proprietary)**



Title: Detection of Reactor Head Base Metal Loss from Inside the CRDM Penetration		
Key Words: Technical Justification	Date: 8/14/03	Document Number: WDI-TJ-001-02-NP Rev.2

Westinghouse Non-Proprietary Class 3

Author(s): Zoran Kuljis <i>Rev. 1.0 F.R. Zoran Kuljis 08.14.03</i>	Cognizant Manger: Don Adamonis <i>Don Adamonis 8/14/03</i>								
Customer	<table border="1"><tr><td>Required</td><td><input type="checkbox"/></td><td>Yes</td><td><input type="checkbox"/></td><td>No</td><td><input type="checkbox"/></td><td>Date</td><td><input type="checkbox"/></td></tr></table>	Required	<input type="checkbox"/>	Yes	<input type="checkbox"/>	No	<input type="checkbox"/>	Date	<input type="checkbox"/>
Required	<input type="checkbox"/>	Yes	<input type="checkbox"/>	No	<input type="checkbox"/>	Date	<input type="checkbox"/>		

Detection of Reactor Head Base Metal Loss from Inside the CRDM Penetration

Introduction

In February of 2002 significant loss of the base metal of the reactor head was discovered at David Besse Nuclear Power Station. The material loss was the result of Boric Acid corrosion of the carbon steel. The particular region of the head where the corrosion had taken place was not identified by visual inspection.

ANO has limited access to the outside surface of the head. As such a program was instituted to develop an inspection that can detect the presence of the carbon steel base metal of the head adjacent to a CRDM penetration. The available examination surface is the inside of a CRDM penetration. The technique chosen as having the highest probability of success was a low frequency eddy current technique.

Technique Description

The CRDM penetrations are of a non-magnetic NiCrFe alloy and the head base metal is a magnetic low alloy carbon steel. The magnetic properties associated with the head base metal offer a means to determine its presence adjacent to the penetration. The simplest inspection to implement for detecting the presence of magnetic is with the use of eddy current techniques.

Eddy current techniques rely on an Electro-magnetic field generated by a coil to interact with a part under test. This applied field generates eddy current flow in the part and this in turn alters the electrical impedance the coil. The Electro-magnetic properties of the part determine the strength and type of interactive response experienced by the coil. For the detection of the base metal of the head adjacent to a CRDM penetration, a coil configuration operates at a low frequency is required to assure that the coil's Electro-magnetic field extends through the CRDM penetration tube. The probe selected for its compatibility with the existing scanner and eddy current instrumentation is a low frequency, driver/pick-up coil probe. In this probe, the driver and pick-up coils have coincident axes that are placed such that they are oriented radially with respect to the penetration.

To perform the inspection, the eddy current probe is mounted into a tool that scans the probe on the ID surface of the penetration over an extent coincident with the head base metal. Figure 1 shows the probe mounted in a sled on the scanning tool. As the probe is scanned over the area of interest a loss in the base metal is detected as a change in the response of the coil.

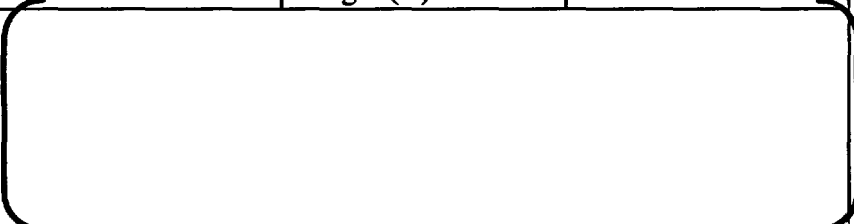
Technique Evaluation

After a series of bench top tests, the eddy current probe selected for evaluation is a ¾ inch diameter driver/pick-up probe (DP-750-SP). The probe was operated at an inspection frequency of 200 Hz. The

probe evaluation was conducted with the probe mounted in a 7010 manipulator. The evaluations were conducted using a head from cancelled reactor located at the Westinghouse Waltz Mills and machined samples. These tests were aimed at understanding the parameters governing the response to the material loss and the "noise" associated with field implementation. The scan increments, reference sensitivities etc. were in accordance with the parameters in the procedure WDI-ET-005.

Figure 2 shows the samples that were machined for this evaluation. They include two material loss morphologies. The first is uniform loss that is simulated by rings cut into the inside of a hollow cylinder. The second is localized loss that is simulated by axially oriented grooves cut into the inside of a half-cylindrical section. Table 1 lists the nominal dimensions for all of these samples. The samples in Table 1 were machined to fit the CRDM penetration tube R 6517-2 with an outside diameter of 4.10 inches and a wall thickness of 0.685 inch.

Table 1 Simulated loss dimensions in machined samples

Sample	Axial Length (in)	Circumferential Length (in)	Radial Depth (in)
SK-WB020408-1/A			
SK-WB020408-1/B			
SK-WB020408-2/A			
SK-WB020408-2/B			
SK-WB020408-3/B			
SK-WB020408-2/A			

As a further check on inspection sensitivity an additional sample was fabricated from a section of pipe that was bored to fit over a penetration of 4.150 inch diameter. The resulting tube had an approximately $\frac{1}{4}$ inch thick wall into which two through holes of { } were drilled (Figure 3).

Tests using the machined samples were performed either on a test stand or with the samples surrounding a penetration tube on the head. Figure 4 shows two of the half cylinder samples mounted in the test stand. Figure 5 shows the ring sample (SK-WB020408-3) mounted on a penetration on the head.

Results

Machined Samples

The first tests performed were designed to determine the sensitivity of the inspection to a loss of carbon steel adjacent to a penetration. In these tests the half cylinder sample sections were clamped together and placed over the penetration in the test stand. Figure 6 shows the results of the test. Arrows in the figure indicate the location where responses from the various grooves are anticipated. As can be seen in

the figure only the [a.c.e] has a poor detection resolution in the C-scan presentation. Additional detection resolution (S/N ratio > 3) is achievable with evaluation of the Lissajous signals the response from the 1/4 inch wide by 1/8-inch deep, 3/16 inch deep, 3/16 inch deep, and 1/4 inch deep groove (SK-WB020408-1/B, 2/A, and 2/B). Only the shallowest [a.c.e] produced a weak signal response (S/N ratio < 1) and has remain in practically undetectable signal response range. From these results it was concluded that the total volume of material lost is governing the signal responses.

A supplemental test was conducted to evaluate the sensitivity of the loss response to the area presented to the probe. Two of the half sections were mounted end to end on the test stand. The two sections were then separated at various increments. Measurements of the coil response associated with the gap between the samples were taken. This test duplicates the response of a very long deep loss of various widths. Figure 4 shows the position of the two samples at their maximum separation. The results of these measurements are found in Figure 7. As expected, the ability to detect the presence of the gap falls dramatically, as the width (area) becomes small. As the gap width increases the change in response saturates when [a.c.e]

The final test performed with the machined samples on the test stand determined the dependence of the coil response on the radial depth of material loss. To simulate this type of loss, shims were placed under the upper half section shown in Figure 3. This gives an approximation to the rings machined into Sample SK-WB020408-3 (A and B) but with more flexibility in terms of radial dimension. The measurements consisted of taking the difference in the amplitude of the vertical component of the eddy current response at approximately 1.5 inches within each sample on the same scan line. The measurements from four scan lines were then averaged for the final result. The results of these measurements are found in Figure 8. As a check on the validity of the approach the response of the two grooves in Sample SK-WB020408-3 (A and B) displayed in Figure 9 are shown in Figure 8 as the triangles.

James Port Head

Inspections were performed on six penetrations in the James Port reactor head. This head is from a cancelled plant. All of the displays for these inspections can be found in Appendix A. In general the variations seen in the head inspection are smaller than the variations observed in the machined samples. This fact allows for the counter bore at the top of the head to be observed. The counter bore is a radial opening of the hole in the head through which the penetration is inserted. The counter bore extends over the portion of the hole that is on the "high" side down to the "low" side. Figure 10 shows the results from Penetration 26 with the counter bore obvious in the display.

A further test was conducted where the 1/4 inch thick tube sample with the two holes through the wall was slipped over a penetration that had been cut-off. The results of this inspection are found in Figure 11. Again as with the counter bore the presence of the [a.c.e]

Discussion

In reviewing the results the variations in response observed in the machined samples figure 9 is significantly (two times) higher than that observed in the head Figure 10. The origin of the variation has not been definitively identified but is believed to originate with a combination of material variability with in the penetration tube being used in the test stand and residual magnetic fields within the samples. These variations limit the detection of low level loss. Without these variations the signal to noise should improve allowing the detection level in the head to also improve over that observed in the samples.

The penetrations on the head are slightly smaller in diameter (4.0 inch diameter) than the penetration used in the test stand so that the pipe sample had a gap between the OD of the penetration and the inside of the pipe. This may have contributed to the ^{a.c.e} Bench tests had observed a response for the hole but as expected, at smaller amplitude than the responses of the 1-inch hole.

The results associated with a variation in the gap width (Figure 7) suggest that quantitative measurement of the material loss is indeed possible so long as the area of loss is ^{a.c.e} Further these results suggest that even if the area of loss is smaller, quantitative measurement of the loss may be possible by correcting the measurements (Figure 8) with a factor derived from the gap dependence (Figure 7).

The extension of the inspection to a CRDM penetration tube of slightly different dimensions should not present a significant problem. During this evaluation penetration diameters from 4.0 to 4.15 inches in diameter were considered. As the diameter and wall thickness of a penetration decrease the sensitivity of the inspection will improve and the curve in Figure 8 will become conservative.

Summary

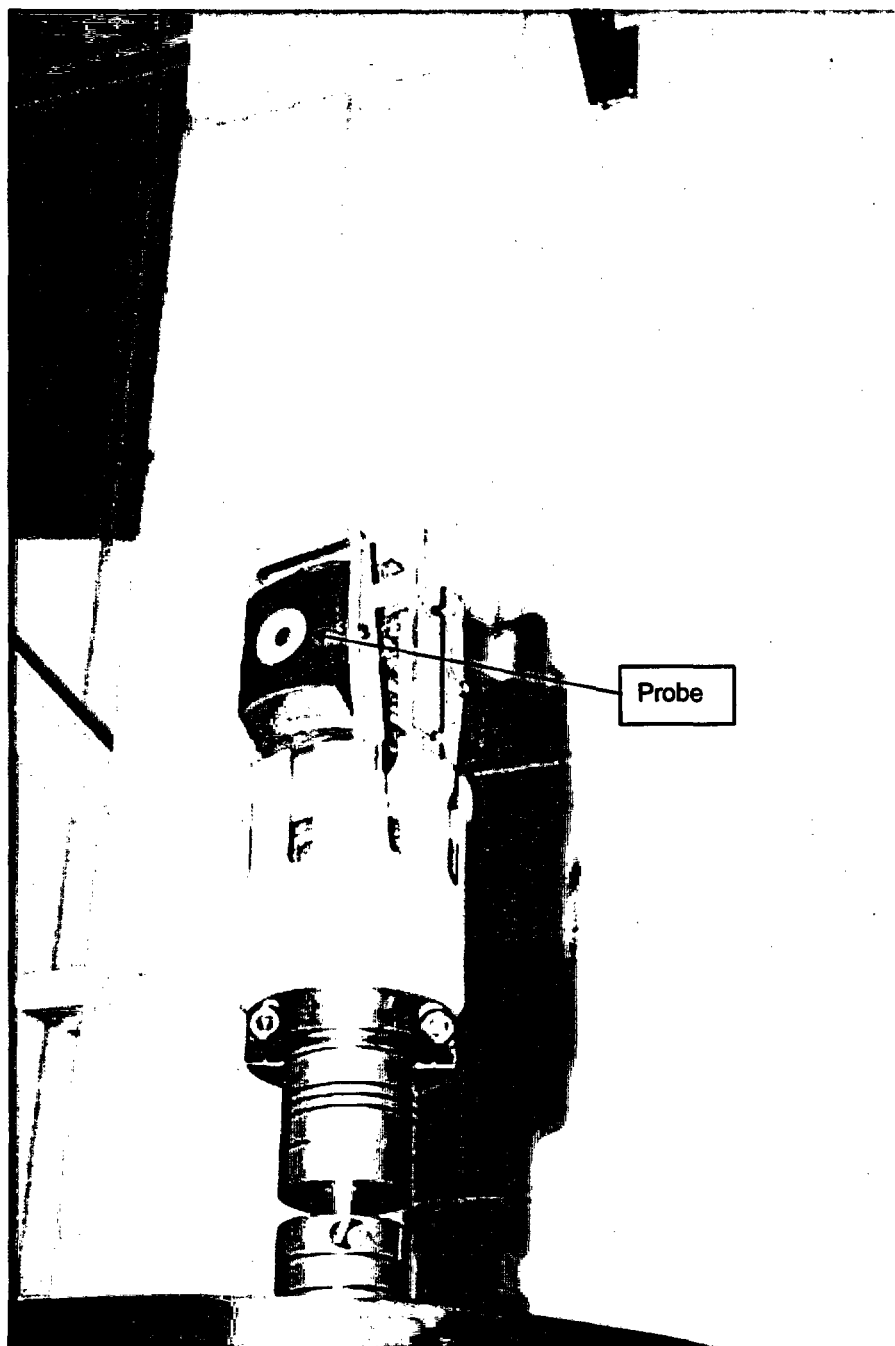
These tests found that the key parameter determining the response of the inspection is the volume of the loss presented to the probe. Three out of four ^{a.c.e}

^{a.c.e} Further the tests on the head found that the material noise was lower than that of the machined samples and that the counter bore at the top of the head could be readily detected. At present the technique is capable of estimating the amount of material lost, so long as it extends over a "wide" area. The measurement is based upon a calibration curve developed by displacing a ring section radially from the OD of the CRDM penetration. For assessing small areas of loss additional work will be required.

References

1. WDI-ET-005, Rev 0, "RPV Head CRDM Penetration EC Examination for Wastage Detection"
-

Figure 1 Eddy current probe mounted in the sled of a 7010 manipulator.



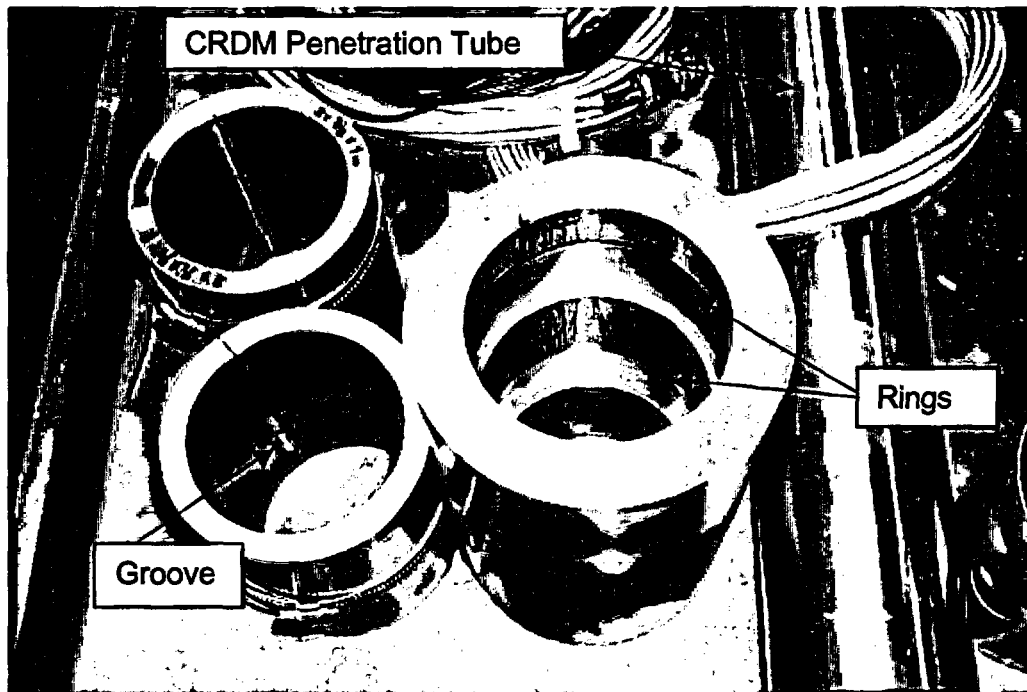


Figure 2 Machined samples used in this evaluation. The samples SK-WB08-1 through - 4 are shown clamped together. The penetration tube was used in the test stand.

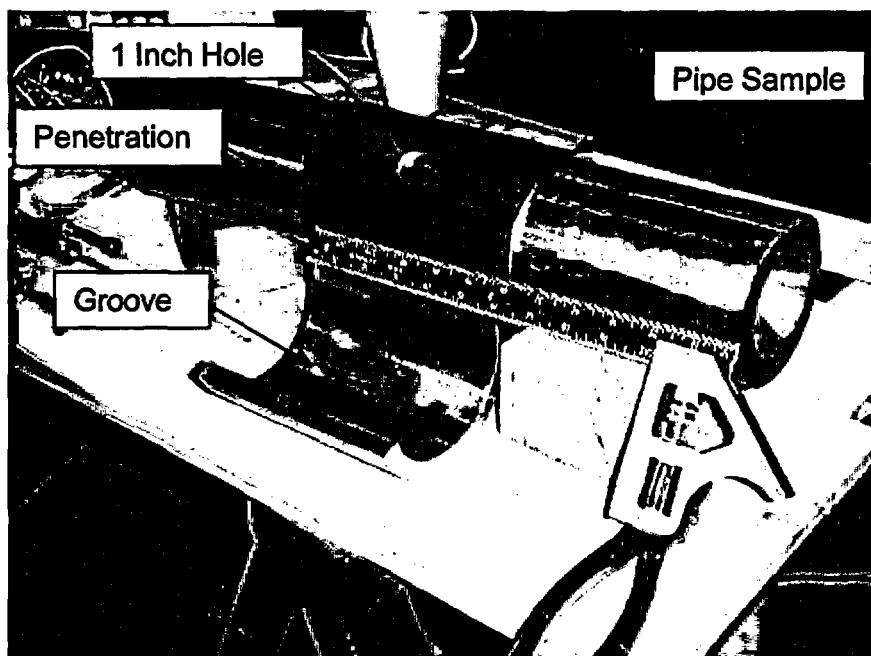


Figure 3 The tube sample with the through wall holes mounted on the penetration tube. In front is the groove Sample SK-WB08-04.

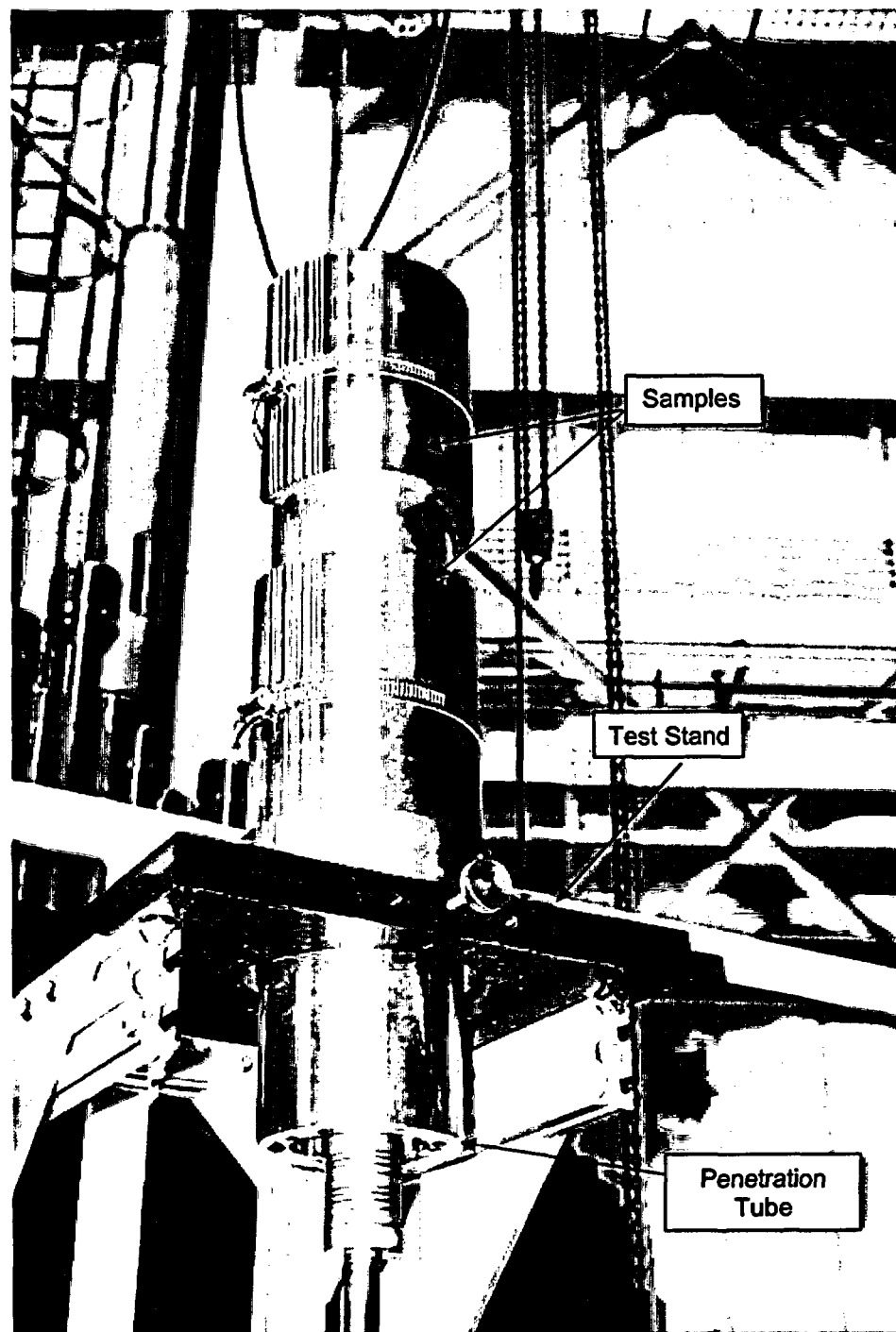


Figure 4 Half Cylinder Samples mounted on test stand. The samples are shown mounted for the “Gap” dependence study and are at the 2.0-inch separation.

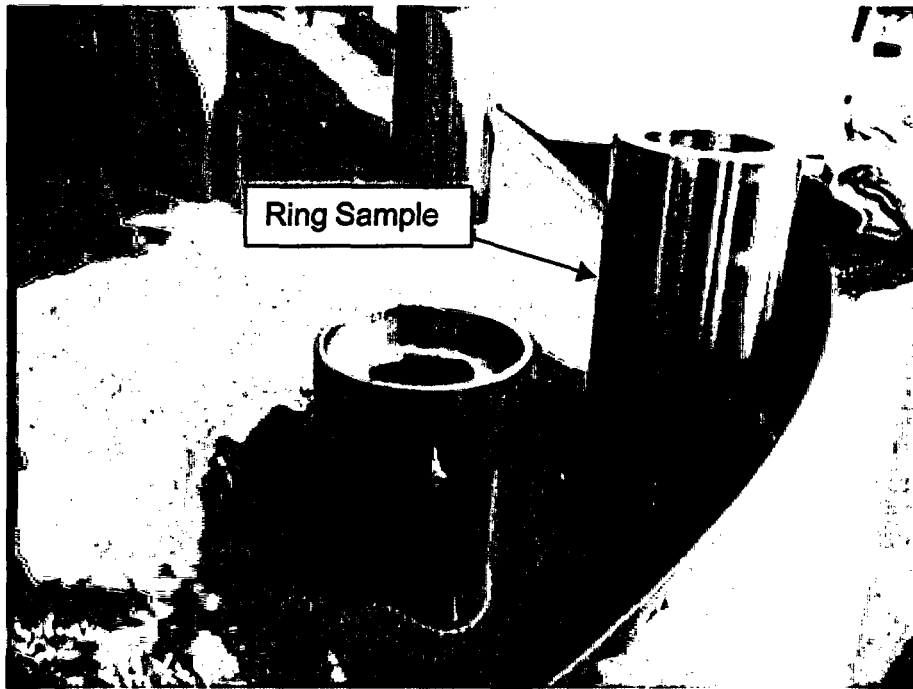


Figure 5 James Port Head with calibration ring and ring sample in position.

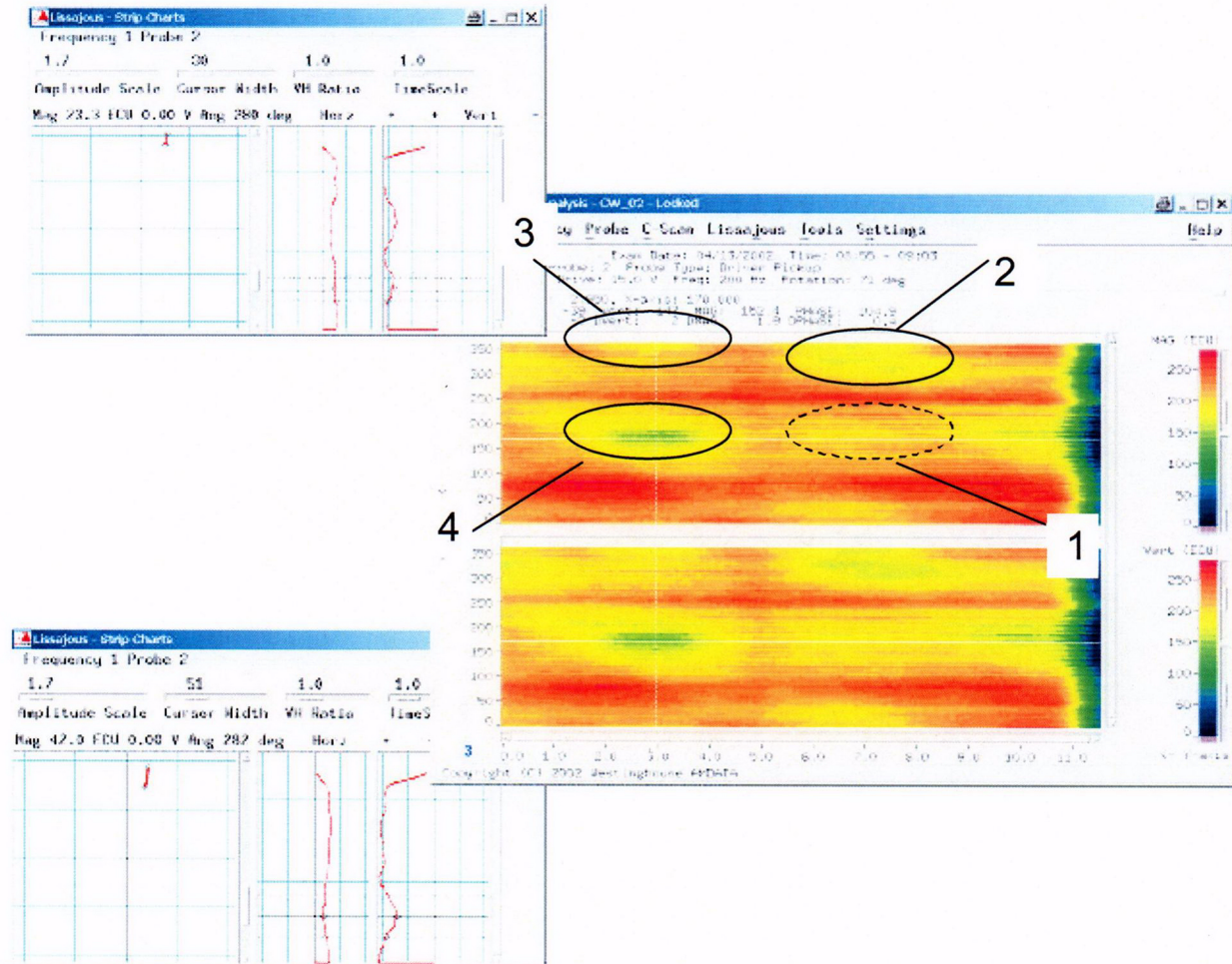


Figure 6

Results from the inspection of the Half Cylinder Samples mounted on the test stand. Arrows indicate location where groove response should be located in the sample identified by the number.

1) SK-WB020408-1/A, 2) SK- WB020408-1/B, 3) SK- WB020408-2/A, 4) SK- WB020408-2/B

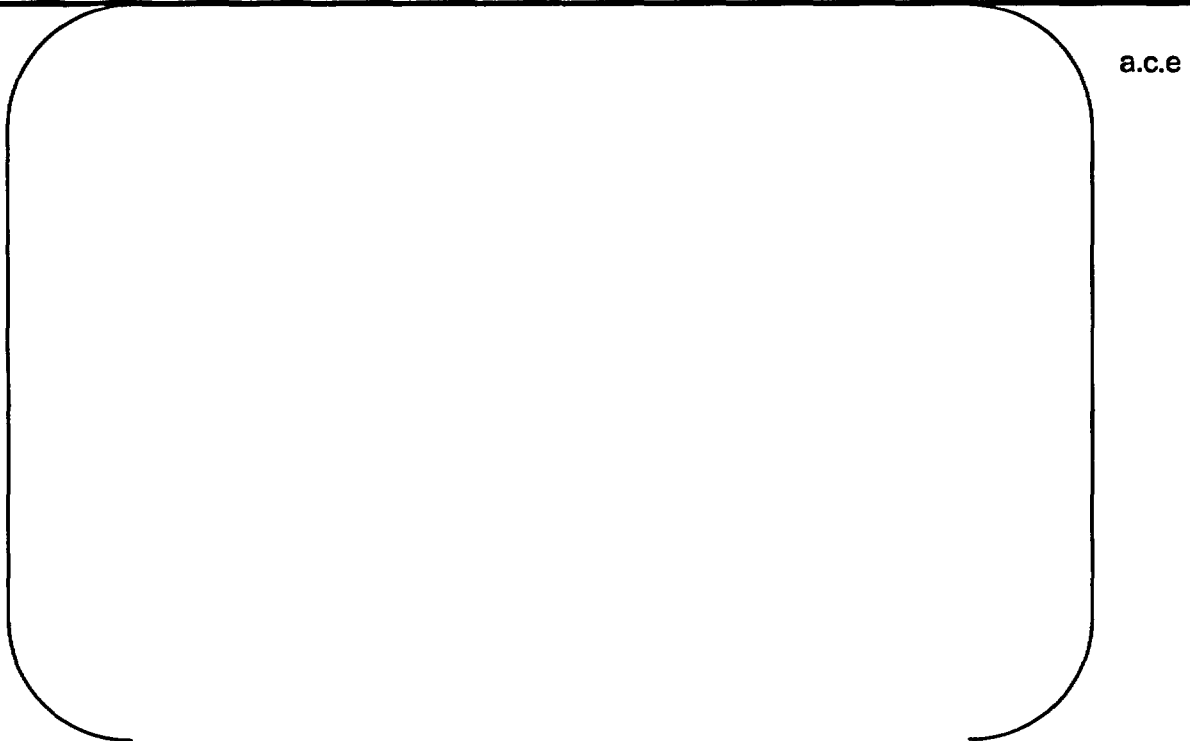


Figure 7 Influence of the width on the reduction in the eddy current response of a long deep simulated loss. Note that the reduction in the response due to the gap saturates when the width is [

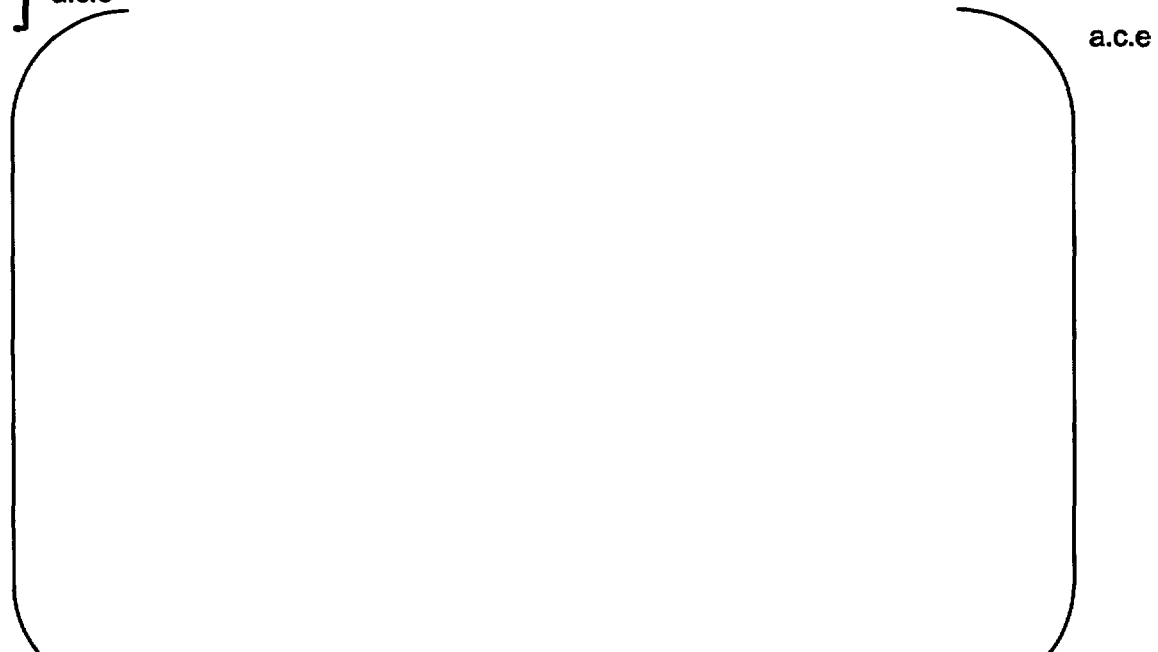


Figure 8 The dependence of the reduction in the eddy current response on the radial loss of the base metal. The squares are the result of placing shims between the OD of the penetration tube and the inside of the half cylinder. The triangles are measurements performed on Sample SK-WB08-5 (A and B).

a.c.e

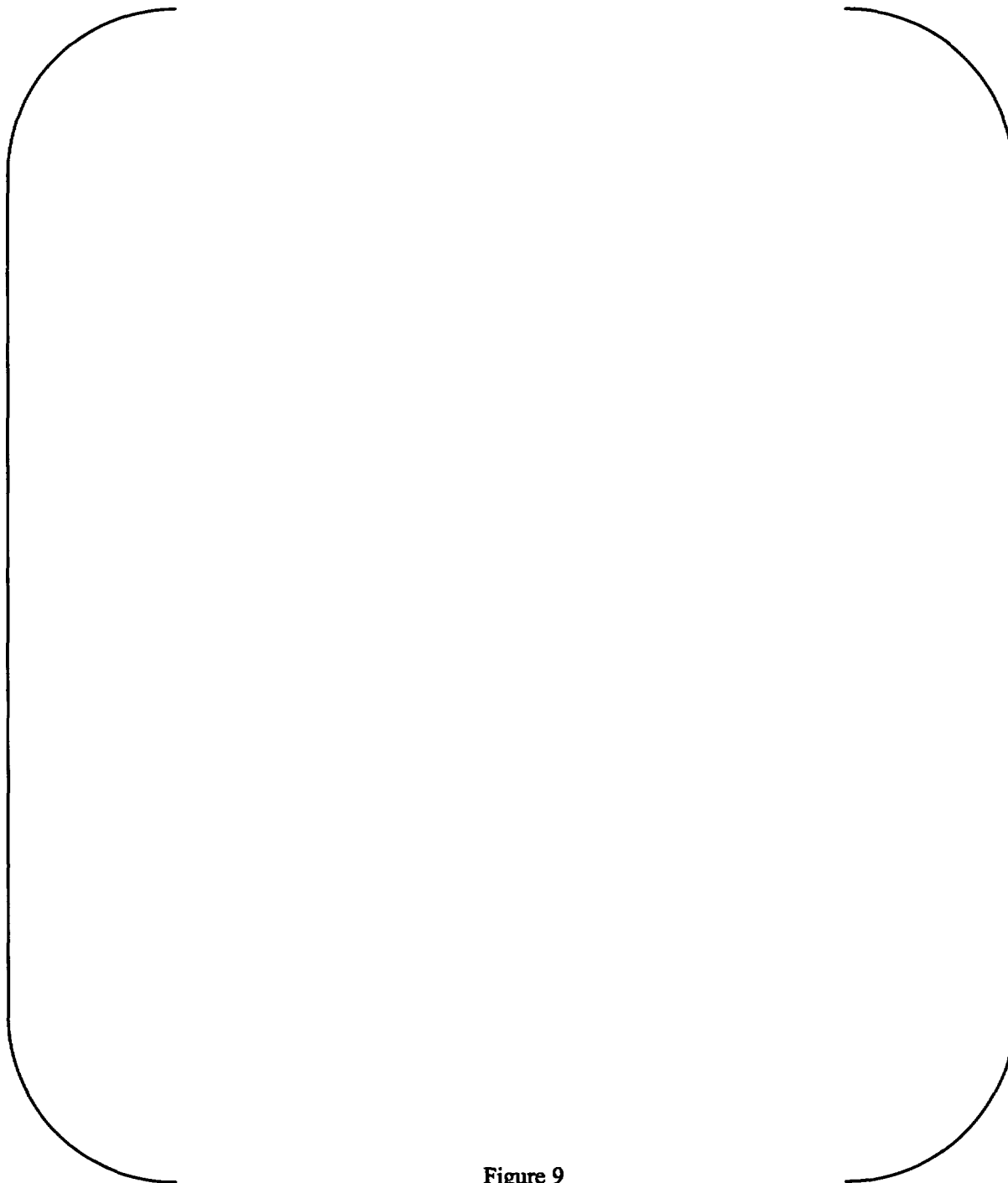


Figure 9
Eddy current response from Circumferential Rings SK- WB020408-3/A and B.

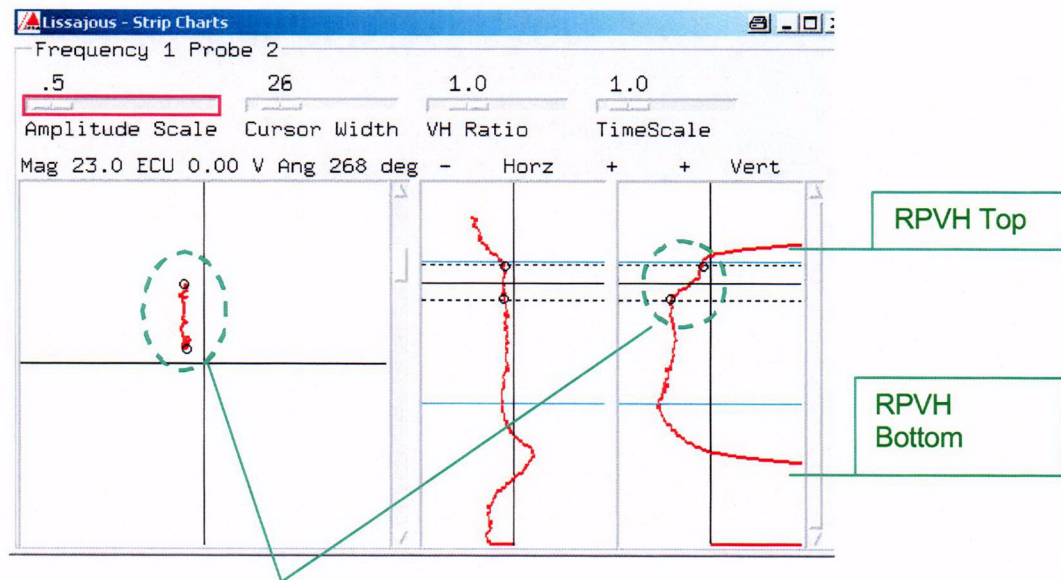
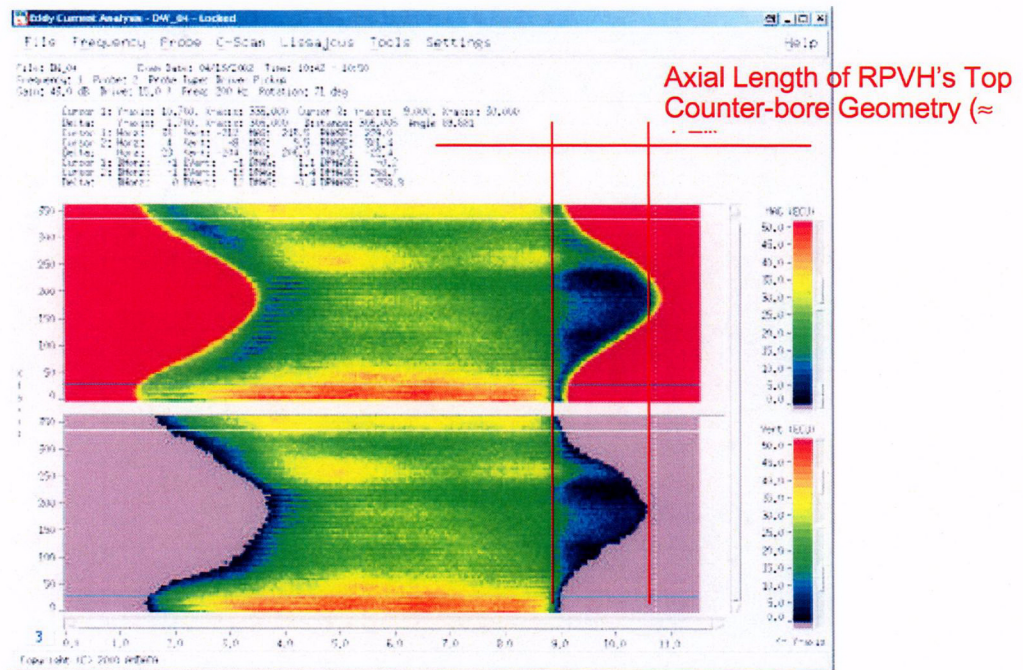
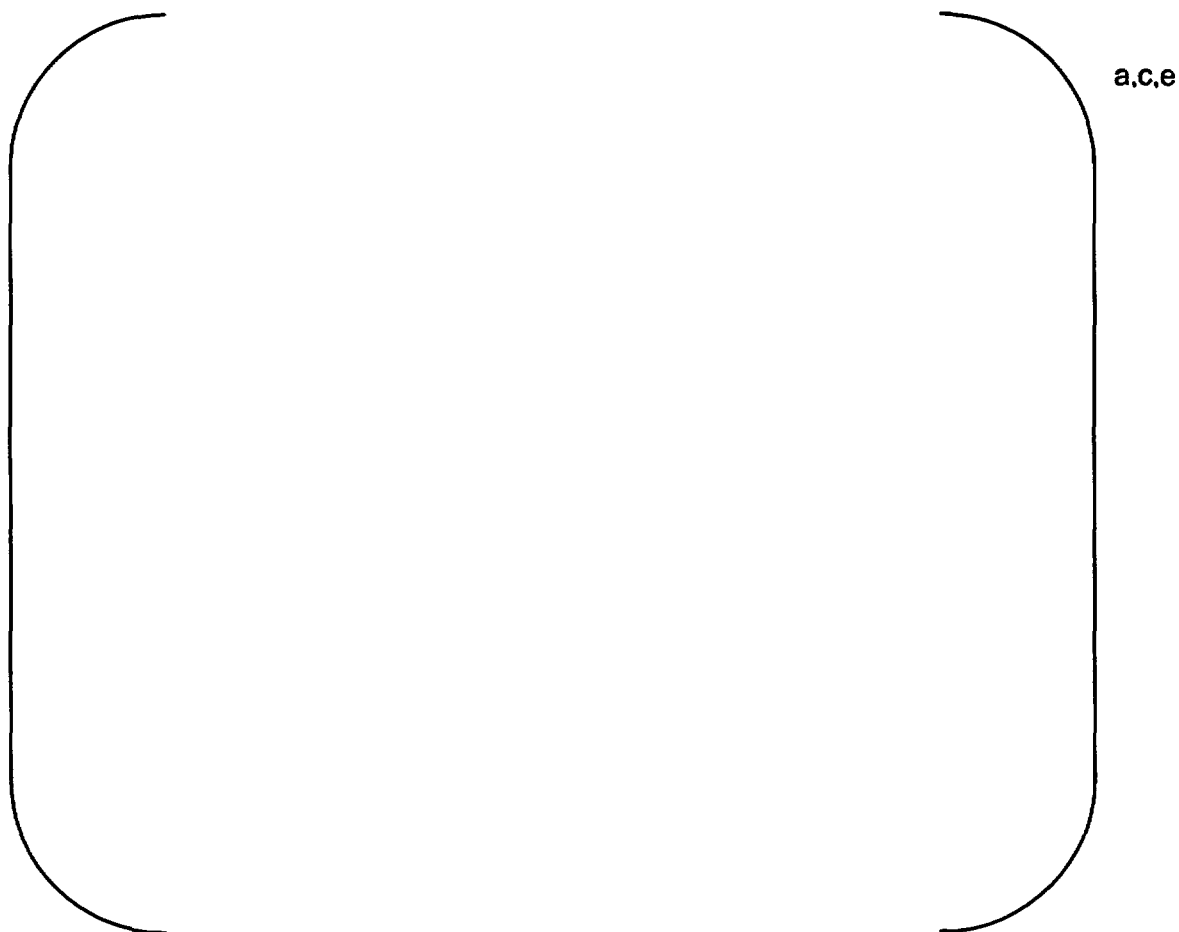


Figure 10

Eddy current responses from inspection of CRDM Penetration 26 in the James Port head. The arrows identify the counter bore region in both the C-Scan and strip chart displays.



Figures 11 Eddy current responses from 1/4 inch thick pipe sample with through wall holes placed on a cut penetration on the head. The response from the [] a.c.e

Appendix A

Graphical displays of data obtained on the James Port Head. Note all presentations are at the same sensitivity level.



Figure A1 Eddy Current Responses from Penetration 2 of the James Port Head.
(Higher ECU represents the presence of carbon steel adjacent to the penetration.)

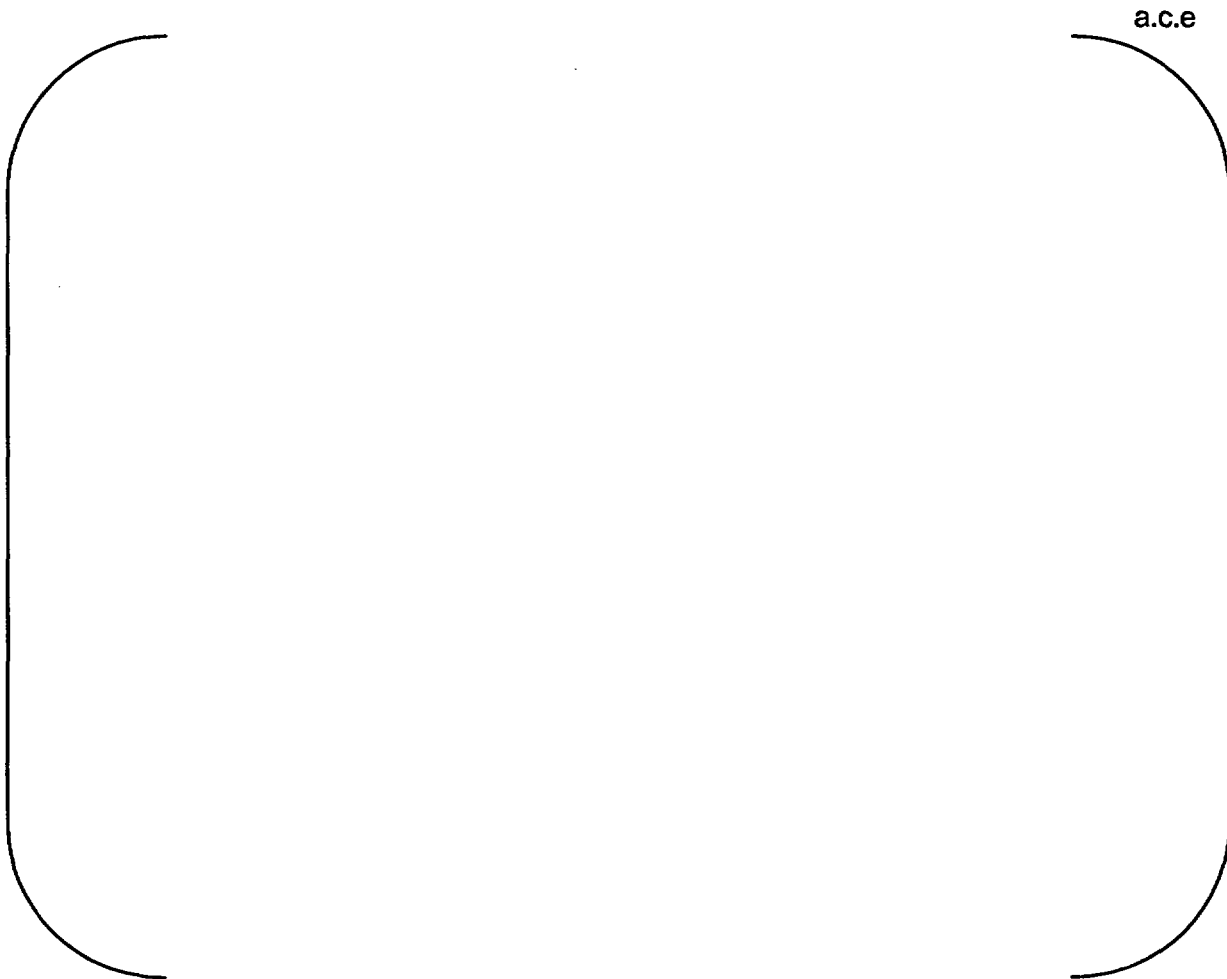


Figure A-2 Eddy Current Responses from Penetration 3 of the James Port Head. (Higher ECU represents the presence of carbon steel adjacent to the penetration.)

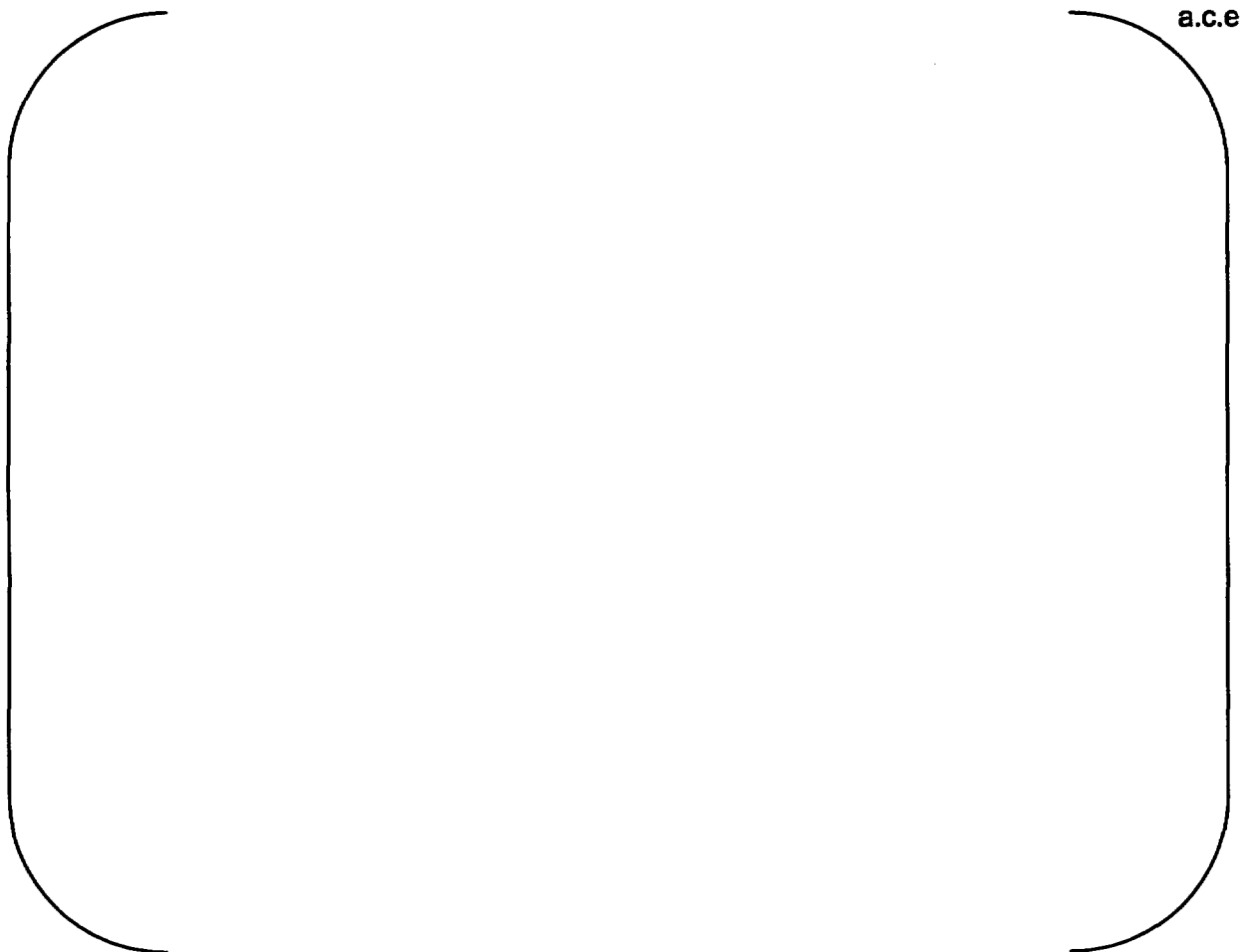


Figure A-3 Eddy Current Responses from Penetration 4 of the James Port Head. (Higher ECU represents the presence of carbon steel adjacent to the penetration.)

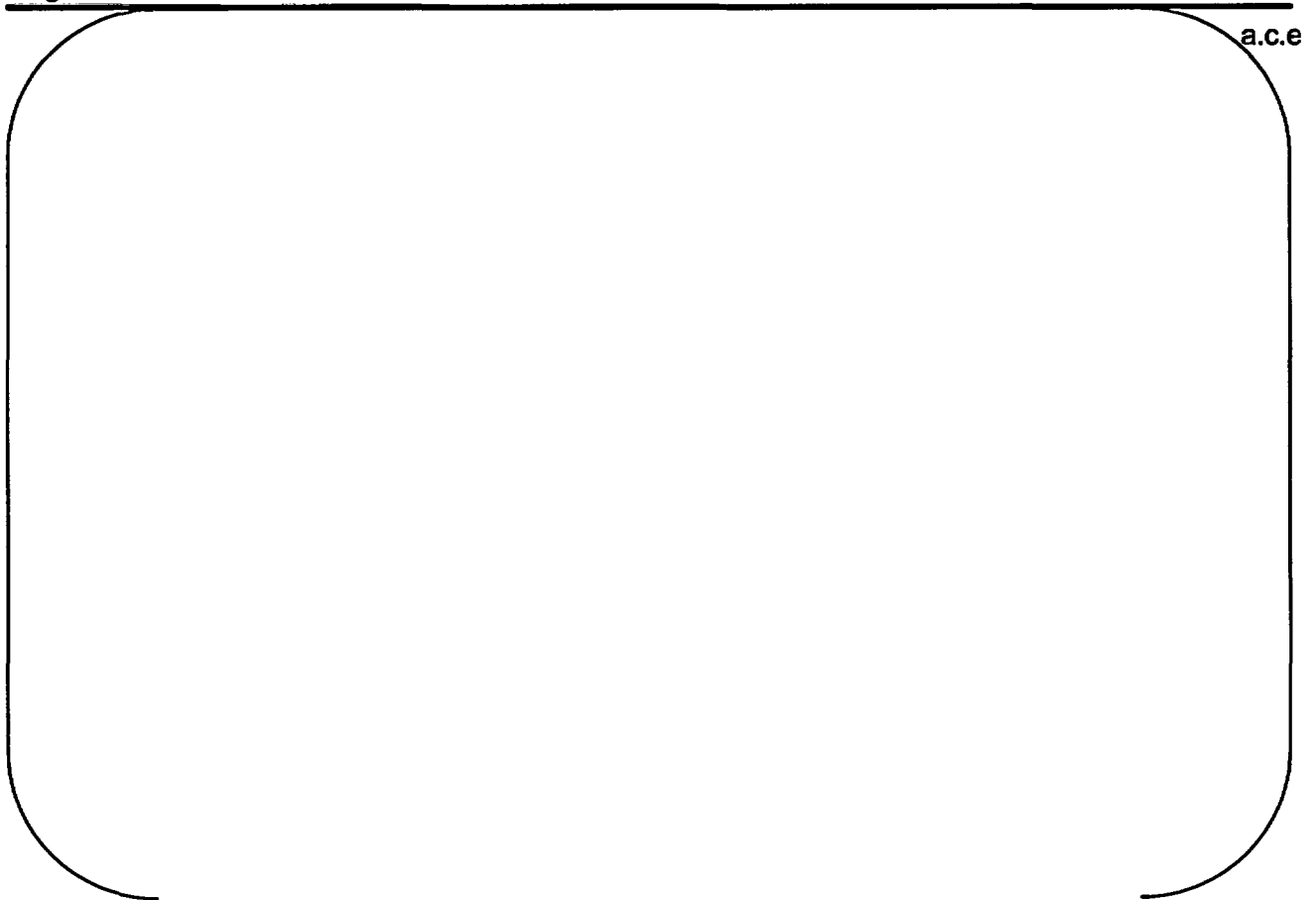


Figure A-4 Eddy Current Responses from Penetration 22 of the James Port Head. (Higher ECU represents the presence of carbon steel adjacent to the penetration.)



Figure A-5 Eddy Current Responses from Penetration 26 of the James Port Head. (Higher ECU represents the presence of carbon steel adjacent to the penetration.)

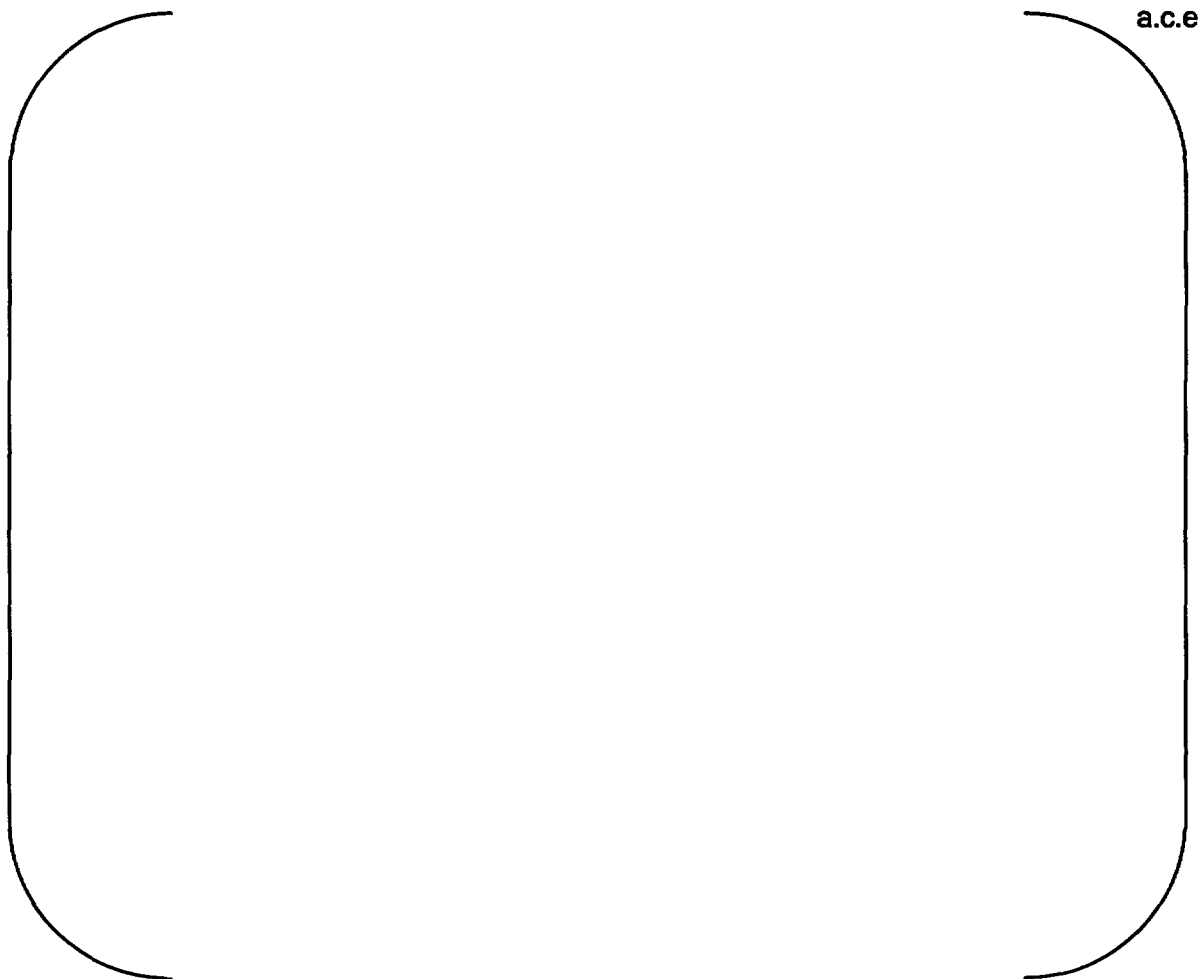


Figure A-6 Eddy Current Responses from Penetration 29 of the James Port Head. (Higher ECU represents the presence of carbon steel adjacent to the penetration.)
